A 3D FINITE ELEMENT MODELING OF HAMMER TEST FOR TRACK PARAMETER IDENTIFICATION

Oregui, M.[1], Li, Z. [1], Dollevoet R. [2], Moraal, J. [1]

[1]*Delft University of Technology, Section of Road and Railway Engineering*
Stevinweg 1, 2628 CN Delft, the Netherlands
E-mail: m.oregui@tudelft.nl

[2]*ProRail, Department of Civil Technology, Asset Management Railsystems*
B4.09, P.O. Box 2038, 3500 GA, Utrecht, the Netherlands

SUMMARY: In railway tracks, short wave rail surface defects give rise to high wheel-rail dynamic forces and noise. Having a better insight into short wave defect occurrence could lead to development of adapted maintenance methods or track design to delay or avoid defect, so that the high short wave defect related maintenance costs may be reduced. As part of a health monitoring method under development, obtaining track dynamic characteristics is the first step in assessing track deterioration. In-situ hammer test measurements are widely used for track parameter derivation. In this paper, in order to reproduce hammer test measurements so that track parameters can be identified, a Finite Element model was developed where the rail and the sleeper were modeled with their real geometry. Although some discrepancy still exists between the first and second order pin-pin anti-resonances and the measured frequencies, the model showed the same main track characteristics in the receptance function as the measurements. The reacceptance function in the frequency range 1500-3000 Hz was also qualitatively determined. The model could not yet simulate the frequency response between 450-1000 Hz for tracks with monoblock and timber sleepers as modal analysis of the sleeper corroborated. Future work is focused on improving the model so that it is valid for the complete frequency range of 450-3000 Hz and tracks of all the sleepers type.

KEYWORDS: hammer test, track vertical dynamics, FE model, parameter identification

1. INTRODUCTION

Railways have been one of the main transport options; metros and trams move millions of people around every day while high speed trains compete with airplanes for journeys of less than 3 hours. This position has been strengthened by the environmentally friendly image of trains.

The increase in speed and axle load of the trains has had a negative effect on the life span of the track systems. Cracks in rails and increase in rolling noise are some consequences of the fast deterioration of track quality. This deterioration is often closely connected to short wave rail surface defects such as poor welds in continuous welded rails, poor insulated joins, short pitch corrugation and squats. Short wave defects can be found in all type of tracks in many world railways where they cause high wheel/rail contact forces [1, 2]. For short pitch corrugation and light squats, the maintenance measure is grinding of the rail top [3]. As severe squats involve deep cracks in the rail and a poor insulated join threatens the safety, costly replacement of the rail or a new insulated join are usually inevitable to avoid a catastrophic rail break [4].

Typical wavelength of short wave defects is between 20 and 80 mm [2, 5, 6]. This wavelength is often independent or weakly dependent upon train speed [7]. In a Dutch main train line with a speed of 140 km/h corresponds to vibrations between 450 and 2000 Hz. This range switches to higher frequencies in high speed train lines. As an example, vibrations almost up to 4 kHz may be reached when trains run at 240 km/h. It appears that the dynamic wheel-rail interaction with this wavelength is very damaging [3, 8].

An approach was proposed based on the comparison of numerical simulations with hammer test measurements for track parameter derivation [9]. The method consists of varying the parameters of a numerical model until the calculated response matches the measurements. The frequency range of interest is limited by the hammer used, which gives reliable data up to 3000 Hz [10]. Once the track parameters are derived, their analysis may lead to a correlation between parameters evolution and defects initiation and growth.

In the beam model of [9], sleepers were approximated as mass points, railpad and ballast as linear spring and viscous damper in parallel, and the rail as a discretely supported beam. The model covered up to 1500 Hz, since the cross-sectional deformation of the rail was not included while it deforms considerably above 1500 Hz affecting the response of the system [11]. Furthermore, sleeper flexibility was not considered so that it could only partially model track with biblock sleeper. Track types of monoblock and timber sleepers were not properly represented because dynamic behavior of the sleepers could not be included (see Figure 1 for sleeper types). Therefore, this paper presents the initial results of a first step in the development of a test method for health assessment and monitoring of track structure conditions. The goal of the current work is to develop a new model valid in the frequency range of interest, 450-3000 Hz, in order to derive parameters from the measurements and to study a possible relation between parameters and defect development. If the evolution of short wave defects is better understood, detection and maintenance measures could be developed. A better understanding could also lead to an improved track design to avoid or delay defect initiation and growth. Any step forward in this field could mean reduction in the high maintenance costs, less disruption to operation of networks, and increase in safety.

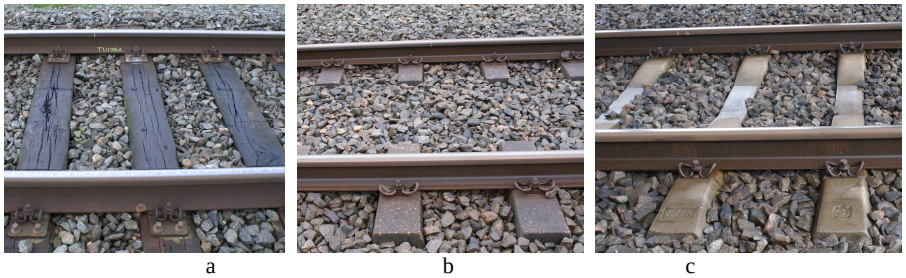

a b c

Figure 1: Railway track with a) timber sleepers b) biblock sleepers, the connecting bars are buried in the ballast c) monoblock sleepers

2. VERTICAL TRACK DYNAMICS

In the frequency range 300-1500 Hz, vertical dynamics of ballasted track are characterized by four features [5]. The first characteristic is a resonance at low frequency called full track resonance; at this frequency the whole track vibrates on the stiffness of the ballast. The resonance is mainly influenced by the subgrade and ballast [12]. The second feature is an anti-resonance, known as sleeper anti-resonance, which corresponds to the movement of the sleeper between rail and ballast while the rail hardly shows any movement. This valley is followed by the so-called rail resonance which takes place due to the antiphase between rail and sleeper. Both sleeper anti-resonance and rail resonance depend especially on rail and railpad characteristics [10]. The forth characteristic of the vertical track dynamics, known as pin-pin anti-resonance, occurs when the rail vibrates with nodes at sleepers, so it is directly related to the sleeper spacing and rail properties. Between 1.5 kHz and 3 kHz, second order pin-pin resonance is found [13].

3. HAMMER TEST MEASUREMENTS IN THE FIELD

Hammer test measurement is one of the techniques used to assess vertical track characteristics, see for instance [14, 15]. Since the frequency distribution depends on the type of track [10, 16], three kinds of tracks with different sleeper types were measured using hammer tests. The tracks had continuous welded UIC54 rail on either concrete (monoblock or biblock) or timber sleepers. At each measurement point, the average of five measurements was calculated so that the random error was minimized. The impact was applied on the rail over the sleeper and the response was measured on the excitation point.

4. MODEL

4.1. Description of 3D Finite Element Model

A 3D Finite Element (FE) model was built to numerically reproduce the hammer test in the time domain. Explicit FE was used so that non-linearities in the system, such as damaged fastening, could also be modeled.

Figure 2a shows the finite element model. As the symmetry of the track about its centre line is applied for vertical track dynamics, only half of the track was considered, see Figure 3a for a 3D overview. As shown in Figure 3b, the rail was modeled with its real geometry so that the cross-sectional deformation was considered. The sleeper was also modeled in 3D. Railpad and ballast were represented as linear spring and viscous damping in parallel. Nominal values of stiffness and damping were taken from [17]. The model was 15 sleeper bays long and rail ends were clamped. The rail was discretely supported with a sleeper distance of 0.6m.

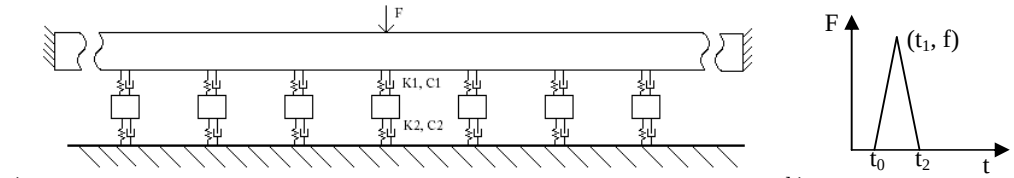

a) b)

Figure 2: a) Overview of the FE model b) Applied force

The impact of the hammer test was simulated as a force applied over the nodes of an area in the middle of the rail. The input force was defined at three points: beginning time (t_0,0), time with the maximum force value (t_1, f) and end time (t_2,0), see Figure 2b. The force f was calculated by dividing the maximum excitation force (F_{max}) with the number of nodes that belonged to the impact area. The values of the parameters t_0, t_1, t_2 and F_{max} were derived from the actual measured impact force of the hammer tests.

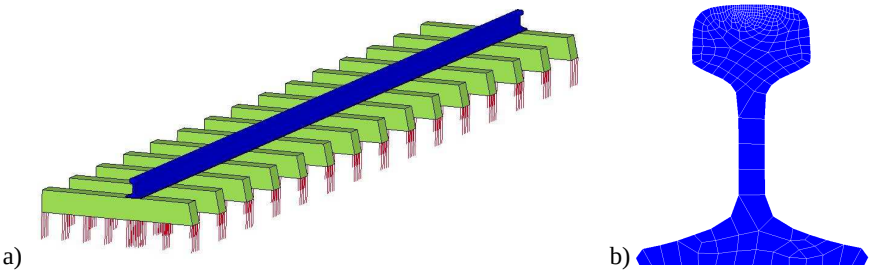

a) b)

Figure 3: a) Overview of the FE model in 3D b) Rail cross-section

4.2. Results

Figure 4 shows the receptance function of three measurements and of a FE model with nominal values of railpad and ballast stiffness and damping, see Table 1. Each measurement corresponds to a different sleeper type track: monoblock, biblock or timber. The three locations do not have a defect on the rail surface and the structure does not seem to be damaged to the naked eye.

Table 1: Ballast and railpad stiffness and damping best fit values

		Nominal	Closest fit	
Railpad	Stiffness, K1 [GN/m]	1.3	1.04	-20%
	Damping, C1 [kNs/m]	45	45	-
Ballast	Stiffness, K2 [MN/m]	45	54	+20%
	Damping, C2 [kNs/m]	32	64	+100%

For tracks with monoblock and timber sleepers, the frequency response functions show different behavior between 450 and 1000 Hz (Figure 4a). The two types of track have a relatively flat receptance function with some variation while the modeling results show one major dip. According to [10], this frequency range is mainly dependent on sleeper and rail characteristics.

Biblock sleepers consist of two blocks of reinforced concrete connected by a steel pipe. In the frequency range 450-1000 Hz, the dynamic behavior of this sleeper is represented in the system receptance function as one anti-resonance at 480 Hz, known as the sleeper anti-resonance. On the contrary, timber and monoblock sleepers are prismatic beams with more resonances and anti-resonances in the same frequency range. Despite the modeling of the sleeper in 3D, the receptance function of the model does not capture the dynamic behavior of the prismatic sleepers in that frequency range.

With regards to both the rail resonance and the pin-pin anti-resonance of monoblock and timber sleeper tracks, the numerically calculated receptance function has peak and valley at 927 and 1298 Hz corresponding to the measurement at 970 and 1100 Hz for monoblock tracks, and 900 and 1080 Hz for biblock tracks. though the positions are displaced. In the case of monoblock sleeper track, an extra dip is noticed at 1310 Hz. For frequencies higher than 1500 Hz, the measured and numerically calculated receptance functions show a similar frequency response where both include a characteristic valley around 2800 Hz, known as the second order pin-pin anti-resonance [13].

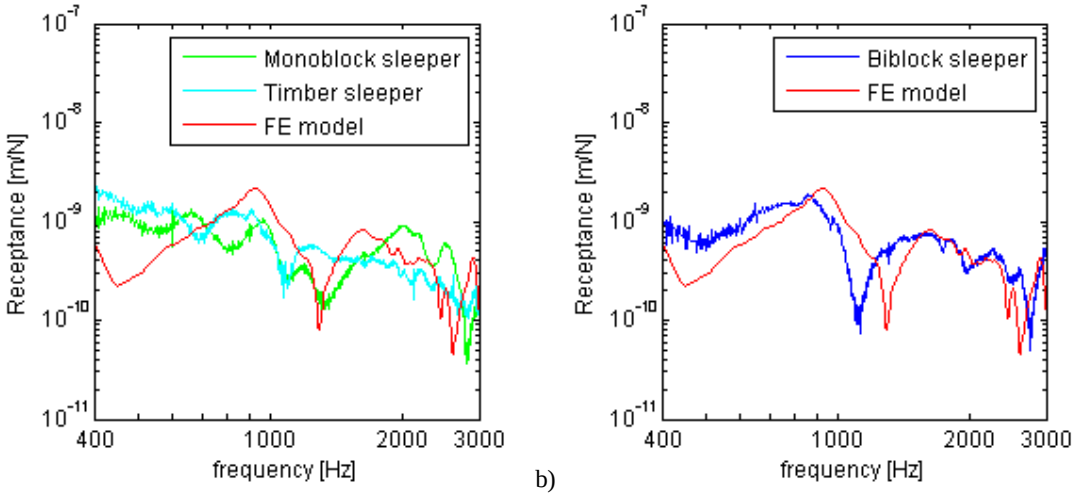

a) b)

Figure 4: Receptance function of measured biblock, monoblock and timber sleeper and a FE model with ballast and railpad stiffness and damping nominal values

In the case of biblock sleepers, although the measured and calculated track characteristics are not at the same frequencies, the characteristic resonances and anti-resonances are recognizable: first the shallow sleeper anti-resonance at 480 and 450 Hz for measured and calculated, followed by the blunt rail resonance at 852 and 927 Hz, then the sharp first order pin-pin anti-resonances at 1111 and 1298 Hz, and the second order pin-pin anti-resonances at 2764 and 2605 Hz. According to previous studies, pin-pin anti-resonance is mainly dependent on sleeper distance [10]. However, although in the FE model the sleepers were modeled every 0.6 meters as in the field, the simulated and measured dips take place at different frequencies. In view of the qualitative agreement between the measurement and the calculation, and the quantitative difference, railpad and ballast parameter study was carried out to fit the four receptance characteristics. Full track resonance was not considered since it takes place out of the frequency range 450-3000 Hz.

The closest receptance function of the FE modeling with respect to the biblock sleeper measurement obtained so far is shown in Figure 5, the corresponding railpad and ballast characteristics are summarized in Table 1. The model can reproduce the receptance function in the frequency range 450-3000 Hz, except the pin-pin anti-resonances. For frequencies higher than 1500 Hz a good duplication of measured valleys and peaks is obtained. After the pin-pin anti-resonance both measured and calculated receptance functions show a peak at 1580 and 1640 Hz respectively. At higher frequencies, three dips are noticed at 1975, 2500 and 2765 Hz for the measurement while at 2040, 2450 and 2615 Hz for the FE model. The last valley corresponds to the second order pin-pin anti-resonance. Variation of the parameters in Table 1 could not lower the pin-pin anti-resonance frequency to the measured one, with the other track characteristics being reproduced in agreement with the measurement. As mentioned in Section 2, pin-pin anti-resonance depends mainly on sleeper distance and rail characteristics. Since the sleeper distance is the same as in the field, rail properties, fastening and railpad modeling are aspects for further study.

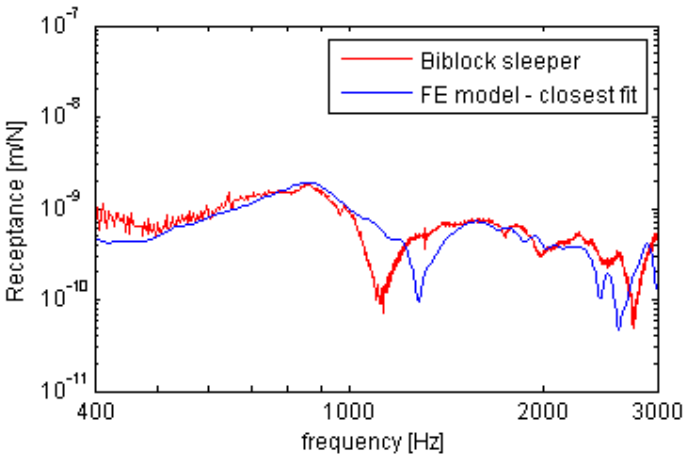

Figure 5: Best fit between biblock sleeper location and the current FE model

5. SLEEPER – MODAL ANALYSIS

Analysis of the results showed that the presented FE model could not reproduce the tracks with monoblock or timber sleeper in the range of 450-1000 Hz where the dynamic behavior of the sleeper plays an important role [10]. In the current model, the sleeper was modeled in 3D with a simplified geometry which could not be able to simulate properly the resonances and anti-resonances of the sleeper. To check how the geometry affects the dynamic behavior of the sleeper, a modal analysis was carried out. The sleeper was studied under free-free conditions, i.e. no restrictions on the boundaries were applied, although Kaewunruen and Remennikov [18] found that the vibration behavior of the sleeper was closely related to the *in situ* conditions which are railpad and ballast characteristics. According to their sensitivity analysis, sleeper's first mode frequency changed about 12% respect to free-free. But in this paper, the first mode was not considered in the parameter identification process since previous studies of sleeper dynamic behavior showed that the first sleeper resonance was usually outside the frequency range of interest [19]. The calculation of the rest of the natural modes in the free-free case compared to *in situ* conditions had an error between 1 and 5% according to [18]. For the current modal analysis, unfortunately measured sleeper natural frequencies were not available for comparison.

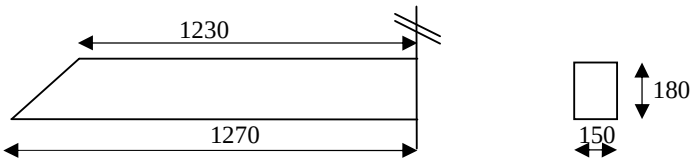

Figure 6: Simplified sleeper geometry [mm]

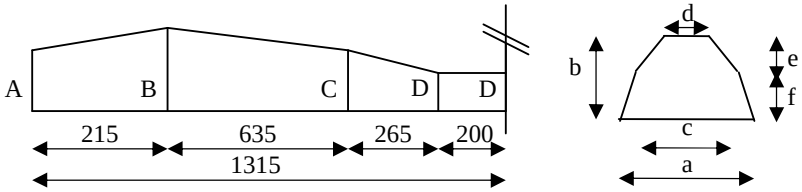

Figure 7: Realistic sleeper geometry [mm]

Two sleeper models were studied: simplified and realistic sleeper geometry. The simplified sleeper was directly taken from the track model of Figure 3 and it was a prismatic beam; see Figure 6 for geometry details. The more realistic representation of the sleeper consisted of four different sections indicated with A-D in Figure 7. The dimensions of the sections are listed in Table 2. For both models two cases were studied. First, the dynamic behavior of a whole sleeper was studied. Second, the resonances and anti-resonances of half sleeper were analyzed since the presented track model only considered half of the track. The symmetry of the sleeper with respect to its centre line was taken into account by restricting the displacement on the longitudinal direction of the sleeper of the nodes on the symmetry plane.

Table 2: Realistic sleeper sections dimensions

	Dimensions [mm]					
Sections	a	b	c	d	e	f
A	300	211	246	148	98	135
B	300	233	246	148	98	135
C	245	225	163.5	143	20	205
D	220	175	150	-	-	-

5.1. Whole sleeper

Figure 8 shows the first four vertical vibration modes of the realistic sleeper while Figure 9 the ones of the simplified sleeper. The natural frequencies are summarized in Table 3. If the results of the two models are compared, the natural frequencies of the simplified model are higher than the geometrically more accurate model.

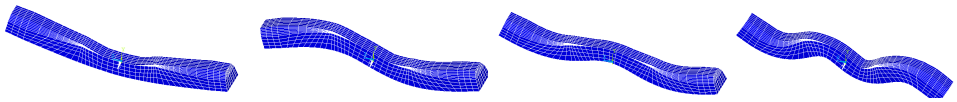

M1 M2 M3 M4

Figure 8: Whole realistic sleeper – the first four vertical mode shapes

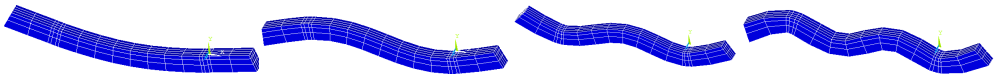

M1 M2 M3 M4

Figure 9: Whole simplified sleeper – the first four vertical mode shapes

Table 3: Natural frequencies of the first four modes of the sleeper models

Mode	Realistic sleeper [HZ]	Simplified sleeper [Hz]	Relative difference with respect to realistic
1st	200	265	32%
2nd	644	710	10%
3rd	1199	1351	12%
4th	1955	2215	13%

5.2. Half sleeper

For vertical track dynamics, the symmetry of the track to the centre line is usually applied. Then, half of the sleeper is modeled, which implies that only the symmetric modes can be represented. Figure 10 shows the modes for realistic and simplified half sleepers. The natural frequencies are the same as the 1st and 3rd mode on Table 3.

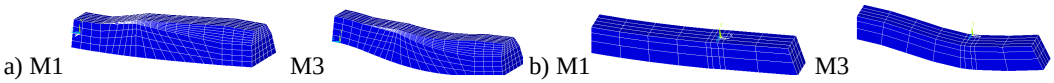

a) M1 M3 b) M1 M3

Figure 10: The first two vertical mode shapes a) Half realistic sleeper b) Half simplified sleeper

5.3 Results

The sleeper modal analysis shows that representing a sleeper by half or whole has significant effect on the response of the system between 450 and 1000 Hz because the sleeper has different dynamic behavior. If half sleeper is modeled, only symmetric modes are included, which is a good representation in the case of biblock sleepers. For monoblock and timber sleepers, the sleepers should be represented in all their length to reproduce all the resonances and anti-resonances of the prismatic sleepers. Future steps will study the effect of including a whole sleeper in the model. With regard to the effect of sleeper geometry, the simplified sleeper is consistently stiffer (10-30%). Although there are not experimental modal analysis of the sleeper values for comparison, the 2nd, 3rd and 4th natural frequencies of the realistic sleeper, 644, 1199 and 1955 Hz respectively, almost agree with the monoblock sleeper track resonances at 660, 1200 and 2000 Hz (Figure 4a). However, the receptance function of the FE model does not show a peak at 1351 Hz. The lack of peak could be because of the difference in boundary conditions between free-free modal analysis and the FE model. This will be further studied.

6. DISCUSSION

6.1. FE model vs. Beam model

The beam model presented in [9] had two main limitations. First, the frequency response function had an upper limit of 1500 Hz because representing the rail as a beam did not include the cross sectional deformation of the rail. To overcome this restraint, the rail was modeled with its real cross-sectional geometry in the current finite element model. Although a perfect reproduction of the measured receptance function was not obtained yet, Figure 5 shows that the FE model followed approximately the measured frequency response function up to 3 kHz. After 1500 Hz, both measured and numerically calculated functions show a qualitative agreement: one peak at 1580 and 1560 Hz for measured and calculated, followed by three dips at 1975, 2500 and 2765 Hz for the biblock sleeper track while at 2010, 2440 and 2615 Hz for the FE model.

The second limitation of the beam model was that tracks with monoblock or timber sleepers could not be represented. Only track of biblock sleeper could be modeled since the sleeper was defined as a mass, which did not include the flexibility of the sleeper. In order to solve this problem, the current FE model included a simplified 3D sleeper. The numerically calculated receptance function and the measurement with biblock sleepers share the receptance function shape: a wide valley at 480 and 450 Hz for measured and calculated and a blunt peak at 852 and 927 Hz. On the contrary, in the frequency range 450-1000 Hz, track with monoblock and timber sleepers showed a peak-valley series that corresponded to the dynamic behavior of the sleeper.

This problem was further studied by performing a sleeper modal analysis which brought insight into the resonances and anti-resonances of the sleeper. If, in the track model, only half of the sleeper was considered, the anti-symmetric modes of the sleeper were no included. For the two sleeper models studied, the first symmetric mode took place around 200 Hz and the next one around 1200 Hz. Therefore, half sleeper did not represent properly the measured frequency response function between 450 and 1000 Hz because the anti-symmetric mode within this frequency range was missing. An improved FE model may include whole sleepers as a step further to model tracks with timber and monoblock sleepers. The modal study also showed a reasonable agreement between the 2^{nd}, 3^{rd} and 4^{th} natural frequencies of the accurate sleeper geometry at 644.1, 1199.3 and 1955.1 Hz and the resonances of the track with monoblock sleeper at 660, 1200 and 2000 Hz. However, the peak at 1351 Hz of the simplified sleeper was not noticed at the simulated receptance function.

For biblock sleeper track, the current FE model gave a good representation since measured as well as numerical receptance functions showed the same four vertical track characteristics. After railpad and ballast parameter variation study, a reasonable agreement was obtained between the calculated and measured receptance function except for the pin-pin anti-resonances (see Figure 5). The simulated pin-pin anti-resonances could not be adjusted to the measured ones by only varying railpad or ballast parameters while still keeping the other characteristics at the measured frequencies.

6.2. Future work

In this paper, an FE model is developed to reproduces hammer test measurements so that track parameters may be derived, and later related to short wave defect initiation and growth. For track with biblock sleepers, the four vertical track characteristics were reproduced where only two were fitted at the measured frequency. The fact that the pin-pin resonance took place at different frequencies for the simulation and the field requires further investigation. Other parameters such as rail properties, fastening and railpad modeling will be studied to fit the calculated pin-pin frequencies to the measured frequencies. For frequencies higher than 1500 Hz, common peaks and dips were noticed between simulated and measured receptance function, their reproduction at the measured frequency will be studied. In the frequency range of 450-1000 Hz, the current model could only simulate track with biblock sleepers. Based on the results of the sleeper modal analysis, next steps should study a model with whole sleepers so that the response of the system includes both symmetric and anti-symmetric resonances of monoblock and timber sleepers. The improved FE model should be able to reproduce all the main track characteristics irrespective of the type of sleeper.

7. CONCLUSION

In order to reproduce hammer test measurements, a finite element model is presented where rail and sleeper are modeled in 3D. On the contrary to a previous beam model, the FE model is shown to have the potential to cover the frequency range of interest for short wave defects between 450-3000 Hz. Modal analysis of the sleeper showed that, since half of the track was modeled, the reproduced dynamic behavior of the sleeper only included

the symmetric modes. As a consequence, the model could not represent track with monoblock or timber sleepers in the frequency range 450-1000 Hz. For biblock sleepers, all four track vertical characteristics were identified where two of them were fitted to measurements. As an exception, the FE model was not able to fit pin-pin anti-resonances to the measured frequency. For frequencies higher then 1500 Hz, the FE model gave a qualitative representation of the measured receptance function. For future steps, an improved finite element model that reproduces all track characteristics regardless the type of sleeper will be developed.

ACKNOWLEDGEMENTS

The 1st author is grateful to The Basque Government of Spain for the contribution to the financing of her PhD study by means of the Programme of the Researchers' Training Grant.

8. REFERENCES

[1] Clayton, P. and Allery, M. B. P., "Metallurgical aspects of surface damage problems in rails", Canadian Metallurgical Quarterly, 21, 1980, pp. 31-46.

[2] Oostermeijer, K. H., "Review on short pitch rail corrugation studies", Wear, 265, 2008, pp. 1231-1237.

[3] Grassie, S. L., "Rail corrugation: Advances in measurement, understanding and treatment", Wear, 258, 2005, pp. 1224-1234.

[4] Li, Z., Zhao, X., Dollevoet, R., and Molodova, M., "Differential wear and plastic deformation as causes of squat at track local stiffness change combined with other track short defects", Vehicle System Dynamics, 46, 2008, pp. 237-246.

[5] Grassie, S. L., Gregory, R. W., Harrison, D., and Johnson, K. L., "Dynamic response of railway track to high frequency vertical excitation", Journal of Mechanical Engineering Science, 24, 1982, pp. 77-90.

[6] Grassie, S. L. and Kalousek, J., "Rail corrugation: characteristics, causes and treatments", Proceedings of the Institution of Mechanical Engineers, Part F: Journal of Rail and Rapid Transit, 207, 1993, pp. 57-68.

[7] Meehan, P. A., Bellette, P. A., Batten, R. D., Daniel, W. J. T., and Horwood, R. J., "A case study of wear-type rail corrugation prediction and control using speed variation", Journal of Sound and Vibration, 325, 2009, pp. 85-105.

[8] Li, Z., Zhao, X., Esveld, C., Dollevoet, R., and Molodova, M., "An investigation into the causes of squats-Correlation analysis and numerical modeling", Wear, 265, 2008, pp. 1349-1355.

[9] Oregui, M., Li, Z., and Dollevoet, R., "Relating track parameter conditions to squat and corrugation initiation and growth", in ISMA2010, Leuven, Belgium, 2010.

[10] de Man, A., "Dynatrack: a survey of dynamic railway track properties and their quality". PhD Delft: Delft University of Technology, 2002.

[11] Thompson, D. J., "Wheel-rail Noise Generation, Part III: Rail Vibration", Journal of Sound and Vibration, 161, 1993, pp. 421-446.

[12] Knothe, K. and Wu, Y., "Receptance behaviour of railway track and subgrade", Archive of Applied Mechanics, 68, 1998, pp. 457-470.

[13] Wu, T. X. and Thompson, D. J., "A double Timoshenko beam model for vertical vibration analysis of railway track at high frequencies", Journal of Sound and Vibration, 224, 1999, pp. 329-348.

[14] Grassie, S. L. and Cox, S. J., "Dynamic response of railway track with unsupported sleepers", Proceedings of the Institution of Mechanical Engineers. Part D, Transport engineering, 199, 1985, pp. 123-135.

[15] Kaewunruen, S. and Remennikov, A. M., "Field trials for dynamic characteristics of railway track and its components using impact excitation technique", NDT and E International, 40, 2007, pp. 510-519.

[16] Vincent, N. and Thompson, D. J., "Track dynamic behaviour at high frequencies. Part 2: experimental results and comparisons with theory", Vehicle System Dynamics, 24, 1995, pp. 100-114.

[17] Hiensch, M., Nielsen, J. C. O., and Verheijen, E., "Rail corrugation in the Netherlands - Measurements and simulations", Wear, 253, 2002, pp. 140-149.

[18] Kaewunruen, S. and Remennikov, A. M., "Sensitivity analysis of free vibration characteristics of an in situ railway concrete sleeper to variations of rail pad parameters", Journal of Sound and Vibration, 298, 2006, pp. 453-461.

[19] Grassie, S. L., "Dynamic modelling of concrete railway sleepers", Journal of Sound and Vibration, 187, 1995, pp. 799-813.